Exploiting Knowledge Management for Supporting Multi-Band Spectrum Selection in Non-Stationary Environments

Bouali, F., Sallent, O., Pérez-Romero, J. & Agustí, R.

Original citation & hyperlink:
Bouali, F, Sallent, O, Pérez-Romero, J & Agustí , R 2013, 'Exploiting Knowledge Management for Supporting Multi-Band Spectrum Selection in Non-Stationary Environments', IEEE Transactions on Wireless Communications, vol. 12, no. 12, pp. 6228 - 6243. https://dx.doi.org/10.1109/TWC.2013.101713.130165

DOI 10.1109/TWC.2013.101713.130165
ISSN 1536-1276
ESSN 1558-2248

Publisher: Institute of Electrical and Electronics Engineers

Exploiting Knowledge Management for Supporting Multi-Band Spectrum Selection in Non-Stationary Environments

F. Bouali, O. Sallent, J. Pérez-Romero, R. Agustí
Signal Theory and Communications Dept. (TSC)
Universitat Politècnica de Catalunya (UPC), Barcelona, Spain
Email: {faouzi.bouali, sallent, jorperez, ramon}@tsc.upc.edu

***Abstract*—This paper proposes a new knowledge management framework for spectrum selection under non-stationary conditions supporting a set of applications with heterogeneous requirements. In this respect, an optimization problem is formulated to maximize an aggregate utility function that captures the suitability of spectrum portions with respect to the various application requirements and a set of preferences for using the different spectrum bands. Motivated by the practical limitations when solving the considered problem directly, an alternative solution is proposed. It exploits a statistical characterization of the environment retained in the knowledge database of the proposed framework. To cope with non-stationarity of the environment, a reliability tester is proposed to detect relevant changes in radio conditions, and update database statistics accordingly. Then, a knowledge manager exploiting these statistics is developed to monitor the time-varying suitability of spectrum resources. Based on this, a novel spectrum management is proposed to approximate the optimal solution of the considered problem. The results obtained in a realistic digital home reveal that, under stationary conditions, the proposed strategy performs very close to the optimal solution with much less requirements in terms of spectrum reconfiguration and measurement reporting. Furthermore, thanks to the reliability tester support, substantial robustness is shown when interference conditions become non-stationary, thus proving the practicality of the proposed solution.**

I. Context/Motivation

The CR (Cognitive Radio) paradigm has emerged as an intelligent radio that automatically adjusts its behavior based on the active monitoring of its environment [1, 2]. In this context, the introduction of cognitive techniques for the management of wireless networks will lead to enhanced robustness by capitalizing on the intrinsic learning capabilities of cognitive systems. Strengthening these cognitive techniques would be of great interest for optimizing cognitive management functions.

Therefore, the technical requirements of new cognitive management systems have been considered in many studies [3–5]. In particular, many recent proposals have attempted to develop new models and efficient architectures for building new cognitive management systems in emerging environments, such as the Future Internet (FI) [6] or the home environment [7]. The shown usefulness of cognitive capabilities has stimulated the initiation of many research projects (e.g., [8, 9]) and standardization activities (e.g., [10, 11]) to further strengthen and promote the use of cognitive management systems.

The flexibility provided by CR is of paramount importance to enable the so-called dynamic spectrum access (DSA), a new communication paradigm that proposes the use and sharing of available spectrum in an opportunistic manner to increase its usage efficiency. Not surprisingly, this topic has received a lot of interest in the recent literature [12–14]. The flexibility provided by spectrum agility has been materialized in the form of increased efficiency through proper decision-making criteria in the spectrum selection (SS) functionality.

In this respect, we have proposed in [15] and [16] to strengthen the awareness level of CR networks by means of a new fittingness factor concept that captures the suitability of a set of spectrum blocks to support a set of heterogeneous CR applications. Motivated by the shown usefulness of the proposed concept under stationary conditions, this paper aims at extending the proposed framework to cope with a more general setting, where radio and interference conditions may be non-stationary. This extension significantly improves robustness of the proposed solution to support the practical scenarios and use cases recently considered for the application of cognitive systems [17–19], for which the operative conditions are usually non-stationary.

In particular, an optimization problem is formulated in this paper to maximize an aggregate utility function that jointly captures the suitability of the different spectrum portions in terms of fittingness factors and utilization preferences associated with different bands. To tackle the considered problem in a practical way, the first main contribution of this paper is the development of a knowledge management functional architecture for assisting the multi-band spectrum management decision-making process in non-stationary environments. The proposed architecture relies on a knowledge management domain that handles a statistical characterization of fittingness factor values to efficiently monitor suitability of spectrum resources subject to unknown changes in interference conditions, and includes a reliability tester to handle non-stationary interference conditions. The second contribution is the development of a novel spectrum management strategy that approximates the optimal solution of the considered problem. The proposed strategy exploits an estimation of suitability of spectrum resources in relation to application requirements, for assisting both SS and spectrum mobility (SM) functionalities subject to different preferences in using the various spectrum blocks. The third contribution is the assessment of the pro-

posed strategy from both the performance and practicality perspectives in a realistic Digital Home (DH) environment, where radio and interference conditions are non-stationary and a set of constraints have to be fulfilled in using the different bands.

The remainder of this paper is organized as follows. The system model is described in Section II including a Markov chain characterization of observed fittingness factor values. The considered optimization problem is formulated in Section III to maximize an aggregate utility function that jointly captures the suitability of spectrum portions in terms of fittingness factors and utilization preferences. A practical approach to solve the considered problem, based on a new knowledge management functional architecture, is developed in Section IV. Performance evaluation is carried out by means of simulations within a realistic DH environment described in Section V. The obtained results are presented in Section VI, including an evaluation of the performance and practicality of the proposed solution under stationary conditions and an assessment of robustness when conditions become non-stationary. Conclusions are provided in Section VII.

II. System Model

The problem considered in this paper is the selection of the spectrum to be assigned to a set of L radio links that need to be established between pairs of terminals and/or infrastructure nodes. The purpose of the l-th radio link is to support the communication flow generated by a given application (e.g., voice, web browsing, or video call) whose requirements are expressed in terms of a required bit rate $R_{req,l}$ and duration $T_{req,l}$. It is assumed that a central infrastructure node is responsible for managing the communications over the established radio links by assigning the most suitable spectrum resources to each of them depending on the heterogeneous requirements of the applications to be supported. In this respect, the spectrum is modeled as a set of P blocks (denoted as "pools" in this paper), each of bandwidth BW_p. To consider the fact that the different pools may correspond to bands subject to different regulatory regimes and thus have different preferences for utilization, a preference factor $0<\psi^{(l,p)}<1$ is associated with each link/pool pair. The SS decisions made on the infrastructure side are indicated to the various terminal nodes through suitable control channels. It is worth mentioning that the considered centralized setting mainly targets local environments (e.g., digital home) where access to a central point can be relatively easy. Nevertheless, the proposed framework also accepts decentralized or hybrid (e.g., a centralized database for TV whitespace and a decentralized one for ISM band) architectures.

To assess the suitability of spectral resources to meet the heterogeneous application requirements, the so-called fittingness factor ($F^{(l,p)}$) was introduced in [15] as a metric capturing how suitable each p-th spectrum pool is for the application supported by the l-th radio link. $F^{(l,p)}$ assesses the suitability in terms of the bit rate that can be achieved while operating in the spectrum pool p (denoted as $R(l,p)$) versus the bit rate required by the corresponding application ($R_{req,l}$). More specifically, the following fittingness factor function is considered:

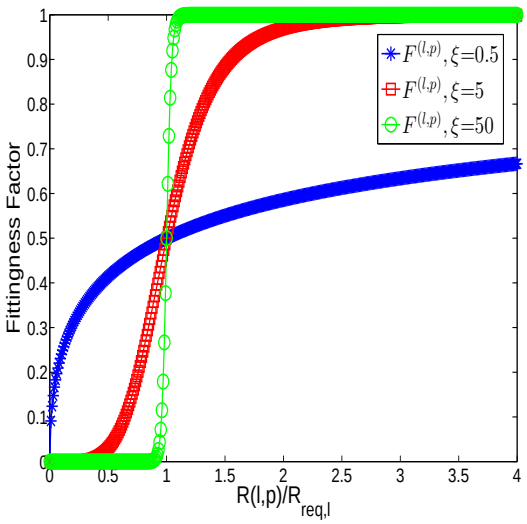

Fig. 1. Fittingness factor behavior

$$F^{(l,p)} = \frac{\left(\frac{R(l,p)}{R_{req,l}}\right)^{\xi}}{1+\left(\frac{R(l,p)}{R_{req,l}}\right)^{\xi}} \quad (1)$$

where ξ is a shaping parameter that allows the function to capture different degrees of elasticity with respect to the required bit rate.

The proposed fittingness factor formulation belongs to the family of sigmoid functions [20]. To better analyse its behavior, Fig. 1 plots it as a function of the ratio $R(l,p)/R_{req,l}$ for different values of the shaping parameter ξ. It can be seen that $F^{(l,p)}$ is a monotonic increasing function of the achievable bit rate $R(l,p)$ that equals 0.5 at $R(l,p)=R_{req,l}$, and tends asymptotically to 1. The marginal increase of the fittingness factor for large bit rates $R(l,p)$ well above the requirement becomes progressively smaller especially when intermediate values of ξ are used (e.g., ξ=5). Therefore, $F^{(l,p)}$ provides a measure of the suitability of a given pool to support link requirements, with values ranging from 0 (low suitability) to 1 (high suitability).

Temporal variations of the fittingness factor will be related with variations in the achievable bit rate due to dynamics of the scenario (e.g, interference variability). To characterize this variability, observed $F^{(l,p)}$ values are quantized into two possible states: 0 (LOW) and 1 (HIGH). The corresponding binary state variable $S_F^{(l,p)}$ is determined, at a given time t, as follows:

$$S_F^{(l,p)}(t)=\begin{cases} 0 \quad (LOW) & \text{if } F^{(l,p)}(t)<\delta_{l,p}, \\ 1 \quad (HIGH) & \text{otherwise.} \end{cases} \quad ;0<\delta_{l,p}<1 \quad (2)$$

where $F^{(l,p)}(t)$ denotes the observed $F^{(l,p)}$ value at time t.

The state $S_F^{(l,p)}$ is assumed to follow a 2-state discrete Markov chain with the following transition probability matrix:

$$\boldsymbol{T_F^{(l,p)}}= \begin{pmatrix} t_{F,0,0}^{(l,p)} & t_{F,0,1}^{(l,p)} \\ t_{F,1,0}^{(l,p)} & t_{F,1,1}^{(l,p)} \end{pmatrix} \quad (3)$$

where $t_{F,k,n}^{(l,p)}$ is the probability that $S_F^{(l,p)}$ switches from state k to state n defined as

$$t_{F,k,n}^{(l,p)}=Prob\left[S_F^{(l,p)}(t+1)=n|S_F^{(l,p)}(t)=k\right] \quad (4)$$

To characterize suitability levels observed in each of these states, $\overline{F_L^{(l,p)}}$ and $\overline{F_H^{(l,p)}}$ are introduced to denote the average $F^{(l,p)}$ values associated with the LOW and HIGH states, respectively. For the sake of brevity, the following vector notation is introduced:

$$\overline{\boldsymbol{F^{(l,p)}}}=\begin{pmatrix}\overline{F_L^{(l,p)}}\\ \overline{F_H^{(l,p)}}\end{pmatrix} \quad (5)$$

III. Optimization Problem

This section considers the problem of assigning the more suitable pools in terms of both fittingness factors $F^{(l,p)}(t)$ and preference factors $\psi^{(l,p)}$ to the set $A(t)$ of active links at a given time t (i.e., links with a communication session in course). In this respect, the following aggregate utility function is proposed to jointly consider both factors:

$$u^{(l,p)}(t)=\psi^{(l,p)}.\overline{\boldsymbol{F^{(l,p)}}}^T\cdot\boldsymbol{diag[\eta_L,\eta_H]}\cdot\boldsymbol{x_F^{(l,p)}(t)} \quad (6)$$

where the vector $\boldsymbol{x_F^{(l,p)}(t)}$ is defined as

$$\boldsymbol{x_F^{(l,p)}(t)}=\begin{cases}(1\ \ 0)^T & \text{if } S_F^{(l,p)}(t)=0.\\ (0\ \ 1)^T & \text{if } S_F^{(l,p)}(t)=1,\end{cases} \quad (7)$$

$(.)^T$ denotes the transpose and $\boldsymbol{diag[\eta_L,\eta_H]}$ is a 2x2 diagonal matrix where the elements $0<\eta_L,\eta_H<1$ of the main diagonal are used for weighting the importance of $\overline{F_L^{(l,p)}}$ and $\overline{F_H^{(l,p)}}$ values in the utility function, thus providing an additional degree of flexibility.

To reflect the assignments that may be performed at a given time t, $d_{l,p}(t)$ is a binary indicator that takes the value 1 if pool p is assigned to link l, and 0 otherwise.

Based on the above considerations, the optimum link/pool allocation at time t will be then the one maximizing:

$$\begin{aligned}&\underset{d_{l,p}(t)}{\text{maximize}}\,(f(d_{l,p}(t)))\\ &\text{subject to:}\\ &\sum_{l\in A(t)}d_{l,p}(t)\leq 1\\ &\sum_{p=1}^{P}d_{l,p}(t)\leq 1\\ &d_{l,p}(t)\in\{0,1\}\end{aligned} \quad (8)$$

where the objective function $f(d_{l,p}(t))$ measures the average utility perceived by active link sessions as:

$$f(d_{l,p}(t))=\frac{1}{|A(t)|}\sum_{l\in A(t)}\sum_{p=1}^{P}d_{l,p}(t)\cdot u^{(l,p)}(t) \quad (9)$$

and $|.|$ denotes the cardinality.

The first constraint in (8) reflects that each pool p can only be allocated to a maximum of one link at time t. The second constraint reflects that each link l can only use a maximum of one pool.

The problem in (8) is a Binary Integer Programming (BIP) problem and more generally an Integer Programming (IP) problem that can be efficiently solved using advanced algorithms, such as branch-and-bound and cutting planes [21]. Nevertheless, as it is formulated, solving the problem would not be practical from two perspectives. On the one hand, it requires to know, at each time t, real values of the state $S_F^{(l,p)}(t)$ of the different pools, which means that $R(l,p)$ values of the different pools should be continuously measured and reported even when pools are not used, and thus would significantly increase the signaling overhead. On the other hand, the optimum allocation should be recomputed at every time t to capture potential changes in interference levels of the different pools.

Therefore, this paper proposes a more practical approach to solve the considered problem. The optimal solution of (8) will be later included in the simulation results as a performance upper bound to assess reliability of the proposed solution.

IV. Proposed Solution

This section develops a solution to efficiently solve the considered optimization problem in (8) by taking into consideration the practical aspects discussed in the previous section. Drawing inspiration from the ETSI-RRS architecture [22, 23], the proposed solution constructs the functional architecture presented in Fig. 2. It includes the following entities:

1) A knowledge management entity is introduced to avoid the need for continuously reporting $R(l,p)$ of all link/pool pairs. In this respect, a knowledge manager (KM) is proposed to estimate the $S_F^{(l,p)}(t)$ state based on a statistical characterization retained in a knowledge database (KD). To keep KD data up-to-date when operating in non-stationary environments, a reliability tester (RT) is constructed to detect relevant changes and restart, when needed, the process of generating KD data.
2) A decision-making entity is introduced to overcome the need for continuously looking for the optimum pool allocation. Instead, the most appropriate pools are assigned to the different links on an event-triggered basis. In this respect, decision-making is split into two functional entities: the SS functionality, which will pick up a suitable pool for each communication whenever a new request for establishing a given link arrives, and the SM functionality, which will perform reconfiguration of assigned pools whenever better pools can be found for some links because of e.g., changes in interference conditions or release of some links. Both SS and SM functionalities rely on the KM support to get the relevant information for the decisions to be made.

In the following, a detailed description of the each of proposed functional modules is proposed.

A. Knowledge management

This section presents the knowledge management modules that monitor the time-varying suitability of spectrum resources to support the considered set of applications.

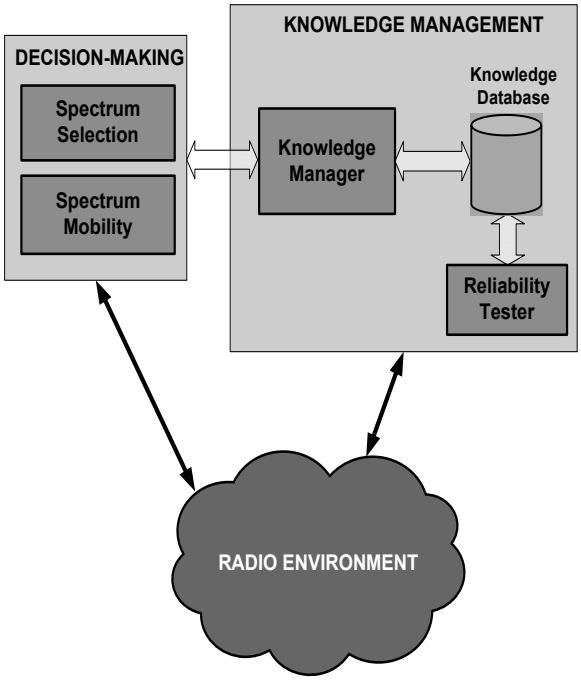

Fig. 2. Functional architecture of the proposed knowledge management framework for SS

1) Knowledge database: To enable a global characterization of the suitability of a given pool p to a given link l based on the history of using this pool, the measurement of $R(l,p)$ of active link/pool pairs will be obtained at each time t, from which the current value of the fittingness factor state $S_F^{(l,p)}(t)$ will be determined and stored in the database, together with a timer $\Delta t^{(l,p)}$ indicating the time elapsed since the measurement was obtained.

Furthermore, assuming a stationary behavior of interference conditions in the different pools, the following statistics are also generated and stored in the KD:

- The transition probability matrix ($\boldsymbol{T_F^{(l,p)}}$).
- The average of observed LOW fittingness factor values:

$$\overline{F_L^{(l,p)}}=E\left(F^{(l,p)}|F^{(l,p)}<\delta_{l,p}\right) \quad (10)$$

- The average of observed HIGH fittingness factor values:

$$\overline{F_H^{(l,p)}}=E\left(F^{(l,p)}|F^{(l,p)}\geq\delta_{l,p}\right) \quad (11)$$

It is worth pointing out that we do not assume any prior knowledge about the above fittingness factor statistics. Instead, they are all constructed based on CR measurements on the environment.

2) Knowledge manager: The KM plays a key role between the knowledge management and decision-making domains of the proposed architecture. It manages the information about the environment retained in the KD to determine the most relevant content for the decision-making entity.

In this respect, the KM retrieves from the KD the transition probability matrix $\boldsymbol{T_F^{(l,p)}}$ together with the value of the fittingness factor state that was stored in the KD $\Delta t^{(l,p)}$ time units ago ($S_F^{(l,p)}(t-\Delta t^{(l,p)})$). Based on this information, the KM first estimates the conditional probability of being in state k at time t given the state $S_F^{(l,p)}(t-\Delta t^{(l,p)})$ $\Pi_{F|F,k}^{(l,p)}(t,\Delta t^{(l,p)})=Prob\left[S_F^{(l,p)}(t)=k|S_F^{(l,p)}(t-\Delta t^{(l,p)}))\right]$ as follows (see proof in Appendix A):

$$\boldsymbol{\Pi_{F|F}^{(l,p)}(t,\Delta t^{(l,p)})}=\left[\boldsymbol{T_F^{(l,p)^T}}\right]^{\Delta t^{(l,p)}}\cdot\boldsymbol{x_F^{(l,p)}(t-\Delta t^{(l,p)})} \quad (12)$$

where $\boldsymbol{\Pi_{F|F}^{(l,p)}}$ is the 2x1 vector of conditional probabilities $\Pi_{F|F,k}^{(l,p)}$ and $\boldsymbol{x_F^{(l,p)}(t-\Delta t^{(l,p)})}$ is defined in (7).

Then, the KM estimates the state $S_F^{(l,p)}(t)$ as follows:

$$\hat{S}_F^{(l,p)}(t)=\begin{cases}0 & \text{with probability } \Pi_{F|F,0}^{(l,p)}(t,\Delta t^{(l,p)}),\\ 1 & \text{with probability } \Pi_{F|F,1}^{(l,p)}(t,\Delta t^{(l,p)}).\end{cases} \quad (13)$$

The KM also identifies changes in estimated states $\hat{S}_F^{(l,p)}(t)$ and informs the decision-making module for its consideration.

3) Reliability tester: As indicated above, the KM exploits the KD content assuming a stationary behavior of radio conditions of the different spectrum pools. In order to make the system robust to unexpected changes, the RT monitors the reliability of stored KD data to identify if the stationary conditions that existed when KD statistics were obtained are still valid. Whenever a relevant change is detected, KD statistics are regenerated under the new conditions.

In this respect, the RT detects relevant changes by monitoring the pools used by active link sessions. A change is judged as relevant if it has a significant impact on the perceived performance by the end-user evaluated in terms of a set of M key performance indicators (KPIs) (e.g., the achievable bit rate $R(l,p)$, the number of spectrum reassignments or spectrum handovers (SpHOs)).

Specifically, the RT procedure computes first, for all $m\in\{1,\ldots,M\}$, an initial estimate of the m-th KPI (denoted as KPI_m) based on its observed sample mean over the established link sessions (let $\overline{KPI_m}$ denote this initial mean estimate). Then, the RT gradually increases the sample window size (denoted as S) as new link sessions are established and updates the observed sample mean ($\overline{KPI_m}$), sample variance ($\overline{\sigma_m}$) and γ confidence interval $\left[\overline{KPI}_{m,min},\overline{KPI}_{m,max}\right]$ defined as the interval that fulfills the following relationship:

$$Prob\left[KPI_m\in\left[\overline{KPI}_{m,min},\overline{KPI}_{m,max}\right]\right]=\gamma \quad (14)$$

Assuming large-sample conditions (typically in the order of $S>30$), $\overline{KPI}_{m,min}$ and $\overline{KPI}_{m,max}$ are given by:

$$\overline{KPI}_{m,min}=\overline{KPI}_m-z_{(1-\gamma)/2}\frac{\overline{\sigma_m}}{\sqrt{S}} \quad (15)$$

$$\overline{KPI}_{m,max}=\overline{KPI}_m+z_{(1-\gamma)/2}\frac{\overline{\sigma_m}}{\sqrt{S}} \quad (16)$$

where $z_{(1-\gamma)/2}=\phi^{-1}(1-\frac{1-\gamma}{2})$ and $\phi(.)$ denotes the normal cumulative distribution function.

Note that as the sample size window S increases, KPI_m tends to converge and the interval $\left[\overline{KPI}_{m,min},\overline{KPI}_{m,max}\right]$ gets narrower.

To achieve a good level of convergence in the initial estimate of KPI_m, the window size S is progressively increased until

the width of the γ confidence interval becomes smaller than a fraction $0<\rho<1$ of the sample mean ($\overline{KPI_m}$), that is:

$$\overline{KPI}_{m,max}-\overline{KPI}_{m,min}<\rho\cdot\overline{KPI_m} \quad (17)$$

Note that decreasing ρ would always improve the asymptotic reliability, but would result in much more time before the condition in (17) is met. Therefore, the smallest value of ρ that would achieve an acceptable level of convergence in each KPI_m can be used in practice. For instance, for the considered scenario in Section V-A, it has been checked that all considered KPIs in Section V-D are achieving a good level of convergence starting from ρ=0.25.

After meeting the stopping rule of (17), $\overline{KPI_m}$ becomes the initial estimate and the current value S of the window size is kept. Then, the RT starts a procedure of monitoring possible changes in the average value of KPI_m based on the statistical technique known in the literature as binary hypothesis testing [24]. Specifically, a null hypothesis (H_0) is introduced to claim that there is no difference between the initial average value ($\overline{KPI_m}$) and a new average value continuously updated based on a moving window of the same size S. Let $\widehat{KPI_m}$ denote this new average value, $\widehat{\sigma_m}$ be its sample variance and $\left[\widehat{KPI}_{m,min},\widehat{KPI}_{m,max}\right]$ be the corresponding γ confidence interval. As long as H_0 holds, KD statistics are assumed to be valid. On the contrary, an alternative hypothesis (H_1) claims that there is a difference between the initial and new average values, and thus KD statistics are no longer valid.

Nevertheless, differences that may be observed between the two average values $\overline{KPI_m}$ and $\widehat{KPI_m}$ do not always imply invalidity of KD statistics, but may be just the result of the pure chance of the experiment. Therefore, the hypothesis testing procedure should ensure with a certain probability that only those differences caused by an actual change in the scenario (e.g., appearance of a new external interferer or change in the position of the transmitter and/or receiver of a given link) are detected. This means, on the one hand, that the probability of selecting H_1 when H_0 actually holds (the so-called Type I error in hypothesis testing terminology [24]) should be kept below a maximum level α. On the other hand, the probability of selecting H_0 when H_1 actually holds (the so-called type II error) should also be kept below a maximum level β.

In general, different detection strategies may be followed to strike a balance between the Type I and II errors. More specifically, it has been shown in [25] that the detection strategy should be designed based on the standardized difference (D_m) between $\overline{KPI_m}$ and $\widehat{KPI_m}$ and the ratio of the largest to smallest sample variance (k_m), defined as

$$D_m=\frac{|\overline{KPI_m}-\widehat{KPI_m}|}{\sqrt{\overline{KPI_m}^2+\widehat{KPI_m}^2}} \quad (18)$$

$$k_m=\frac{max(\overline{\sigma_m},\widehat{\sigma_m})}{min(\overline{\sigma_m},\widehat{\sigma_m})} \quad (19)$$

where the *max(.,.)* and *min(.,.)* functions return the maximum and minimum of two real numbers, respectively.

In this paper, the overlap detection method, that selects H_0 when confidence intervals of the two average values overlap and H_1 otherwise, has been considered. The reason behind this choice is that the considered relevant changes in this paper result in high values of the standardized difference D_m and a ratio of sample variances k_m that is typically close to 1 because both $\overline{KPI_m}$ and $\widehat{KPI_m}$ are determined based on the same window size S. Under these conditions (high D_m and low k_m), the overlap detection method has been shown in [25] to exhibit a very low Type I error and an acceptable Type II error. Consequently, it has been retained in this paper to minimize useless generation of KD data. The reader is referred to Appendix B for a detailed analysis of the overlap detection Type I and II errors.

Algorithm 1 describes the general RT procedure for detecting changes. After testing for changes in each of the converged KPIs in lines 5-11, obtained hypothesis testing results are combined to decide about reliability of the whole KD data according to the procedure described in lines 13-17. Specifically, if H_1 is selected for at least one of the considered KPIs, the combined test selects H_1 (line 14).

Note that the procedure described in lines 13-17 is adequate to detect changes that occur in pools that are used with some regularity by active links. However, it is not valid to detect changes occurring in pools that are never assigned. To overcome this issue, whenever H_0 is selected, the procedure described in lines 18-30 is carried out for each pool that remains unused by any of the considered links for more than a certain period of time named T_Inact. Specifically, a total of N forced measurements are performed to obtain the value of the actual $S_F^{(l,p)}$ state that is compared against the estimate $\hat{S}_F^{(l,p)}$ determined by the KM to test for possible changes (line 25) and select H_1 in case of change (line 26).

The algorithm is concluded by regenerating KD data (line 32) if H_1 is selected following a change in converged KPIs (line 14) or inactive pools (line 26). Then, the RT sets S to zero and loops back to the sequential analysis procedure described in the beginning of the section to recalculate all initial estimates $\{\overline{KPI_m}\}_{1\leq m\leq M}$ under the new conditions (line 33). In this case, the KM will continue using the old KD statistics until the new ones become available.

It is worth mentioning that the combination of individual tests performed by the multiple testing procedure described in lines 13-17 increases in general the Type I error as more tests are combined [26]. To avoid useless generation of KD data, it is proposed to upper-bound the number of KPIs that may be combined to guarantee some Type I error for the whole test (α_{max}) based on the conservative Bonferroni correction [26]:

$$M_{max}=\left\lfloor\frac{\alpha_{max}}{TypeI_{indiv}}\right\rfloor \quad (20)$$

where $\lfloor.\rfloor$ and $TypeI_{indiv}$ denote the floor function and Type I error of each individual test, respectively.

For instance, by setting α_{max}=0.05, k_m=1, D_m=5 and γ=0.95, (20) yields M_{max}=8.

Note that M_{max} provides an upper bound on the number of KPIs that may be combined associated with the maximum tolerable Type I error (α_{max}). Nevertheless, much smaller

Algorithm 1 The RT procedure of detecting changes

1: **for** $m = 1 \rightarrow M$ **do**
2: **if** condition in (17) holds for KPI_m **then**
% Checking convergence of KPIs
3: $Converge(KPI_m) = TRUE$
4: **end if**
5: **if** $Converge(KPI_m) = TRUE$ **then**
% Individual Tests for converged KPIs
6: **if** $\left[\overline{KPI}_{m,min}, \overline{KPI}_{m,max}\right] \bigcap \left[\widehat{KPI}_{m,min}, \widehat{KPI}_{m,max}\right] = \emptyset$ **then**
7: Select H_1;
8: **else**
9: Select H_0;
10: **end if**
11: **end if**
12: **end for**
13: **if** H_1 is selected for at least one KPI_m **then**
% Multiple Testing for detecting changes
14: Select H_1;
15: **else**
16: Select H_0;
17: **end if**
18: **if** (H_0 is selected) AND ($\Delta t^{(l,p)} > T\_Inact$) **then**
% Detecting changes in inactive pools
19: **for** $n = 1 \rightarrow N$ **do**
20: Force a measurement of $S_F^{(l,p)}$;
21: **if** $S_F^{(l,p)} \neq \hat{S}_F^{(l,p)}$ **then**
22: $count{+}{+}$;
23: **end if**
24: **end for**
25: **if** $count = N$ **then**
26: Select H_1;
27: **else**
28: Select H_0;
29: **end if**
30: **end if**
31: **if** H_1 is selected **then**
% Perform required updates if a change is detected
32: Regenerate KD statistics;
33: Recalculate $\{\overline{KPI_m}\}_{1 \leq m \leq M}$;
34: **end if**

Type I errors can be obtained in practice. On the one hand, the considered conservative Bonferroni correction assumes the worst case of independent individual tests to guarantee the target α_{max}. This means, whenever tests are dependent, smaller Type I errors are in general observed. On the other hand, by properly selecting the KPIs that are most likely to be altered following the considered changes, it may be enough to combine $M < M_{max}$ KPIs to detect changes with the corresponding decrease in Type I error. For instance, for the scenario considered in this paper, by using the $M = 6 < M_{max}$ dependent KPIs defined in Section V-D, we were able to detect all considered changes with a much smaller Type I error compared to the target α_{max}. General strategies for optimizing the set of combined KPIs are out of the scope of this paper.

Finally, it is worth pointing out that the parameters N and T_Inact that are used by the procedure of lines 18-30 should be properly set to efficiently detect changes in inactive pools. On the one hand, T_Inact should be longer than the inter-assignment time of pools to the different links in the considered scenario. On the other hand, N should strike a balance between speeding up the detection procedure (i.e., small N) and minimizing the number of Type I errors that may occur (i.e., by wrongly selecting H_1 in line 26) due to the imperfection of the KM in estimating the $S_F^{(l,p)}$ state (i.e., high N). In practice, N should be set to a slightly higher value than the maximum number of consecutive errors that may be made by the KM. In this paper, by setting N=200 and T_Inact=10 h, we were able to quickly detect the considered change in inactive pools ($Change\ \#2$ defined in Section V-B) without any additional Type I error.

B. Decision making

The aim of the SS decision-making process is to allocate, for a given link l, the best spectrum pool $p^*(l)$ among the list of available pools (Av_Pools), i.e., those that are not currently assigned to any other link, to support the corresponding application. To jointly consider the instantaneous utility achieved at link establishment ($u^{(l,p)}(t)$) and the changes that may arise along the link session duration $T_{req,l}$, the following proactive criterion is proposed:

$$p^*(l) = \arg \max_{p \in Av\_Pools} \left(g(\hat{S}_F^{(l,p)}(t), T_{req,l}) \right) \tag{21}$$

where the function $g(\hat{S}_F^{(l,p)}(t), T_{req,l})$ estimates the average utility along the session duration as follows (see proof in Appendix C):

$$\begin{aligned} g(\hat{S}_F^{(l,p)}(t), T_{req,l}) &= \frac{1}{T_{req,l}} \sum_{k=1}^{T_{req,l}} E\left[u^{(l,p)}(t+k) | \hat{S}_F^{(l,p)}(t) \right] \\ &= \frac{\psi^{(l,p)}}{T_{req,l}} \cdot \overline{\boldsymbol{F^{(l,p)}}}^T \cdot \boldsymbol{diag}[\boldsymbol{\eta_L}, \boldsymbol{\eta_H}] \\ &\quad \cdot \left(\sum_{k=1}^{T_{req,l}} \left(\left[\boldsymbol{T_F^{(l,p)^T}} \right]^k \right) \right) \left(\hat{\boldsymbol{x}}_{\boldsymbol{F}}^{(\boldsymbol{l},\boldsymbol{p})}(\boldsymbol{t}) \right. \end{aligned} \tag{22}$$

where

$$\hat{\boldsymbol{x}}_{\boldsymbol{F}}^{(\boldsymbol{l},\boldsymbol{p})}(\boldsymbol{t}) = \begin{cases} (1 \ \ 0)^T & \text{if } \hat{S}_F^{(l,p)}(t) = 0. \\ (0 \ \ 1)^T & \text{if } \hat{S}_F^{(l,p)}(t) = 1, \end{cases} \tag{23}$$

Note that no knowledge about the actual radio conditions experienced in the different pools is required at link establishment because the selection decision is based solely on the estimation $\hat{S}_F^{(l,p)}(t)$ provided by the KM.

Based on the proposed selection criterion, both SS and SM functionalities of the decision-making process are described in the following. In what follows, the time parameter t will be dropped from the $\hat{S}_F^{(l,p)}(t)$ notation for the sake of brevity.

1) Spectrum Selection: The proposed fittingness factor-based SS algorithm is described in Algorithm 2. It is executed every time that the start of a new application requires the establishment of a radio link to support the communication. Upon receiving a request for establishing a link l session, it is rejected if the set of available pools is empty (line 3). Otherwise, estimated $\{S_F^{(l,p)}\}_{1 \leq p \leq P}$ states are obtained from the KM (line 5). Then, the available spectrum pool $p^*(l)$ with the largest $g(\hat{S}_F^{(l,p)}(t), T_{req,l})$ is selected (lines 6 and 7).

2) Spectrum Mobility: The SM functionality attempts to ensure highly efficient allocation of available spectrum pools to each of the established radio links. Therefore, whenever an event that might have influence on the SS decision-making process occurs, the SM will be executed. Such events include

(1) a spectrum pool being released due to finalization of the corresponding application, or (2) a change in the state $\hat{S}_F^{(l,p)}$ of an active link/pool pair being detected by the KM.

As detailed by Algorithm 3, the proposed fittingness factor-based SM algorithm first gets the current $\{\hat{S}_F^{(l,p)}\}_{1\leq L\leq l, 1\leq p\leq P}$ estimates from the KM. The list of active links $A(t)$ is explored in the decreasing order of $R_{req,l}/\overline{R_l}$, where $\overline{R_l}$ denotes the average bit rate observed over previously established link l sessions. This prioritization ordering introduces a fairness criterion that prioritizes both the neediest links (high $R_{req,l}$) and the least-satisfied links (small $\overline{R_l}$). For each link, the reconfiguration decision is based on a comparison between the in use pool ($p^*(l)$) and the currently best pool ($new\_p^*(l)$) in terms of $g(\hat{S}_F^{(l,p)}(t), Rem\_T_l(t))$, where $Rem\_T_l(t)$ denotes, at a given moment t, the remaining time before link session ends. Specifically, if $\hat{S}_F^{(l,p^*(l))}=LOW$ and $\hat{S}_F^{(l,new\_p^*(l))}=HIGH$ (line 7), an SpHO from $p^*(l)$ to $new\_p^*(l)$ is performed because $new\_p^*(l)$ fits better link l. The same occurs if $\hat{S}_F^{(l,p^*(l))}=\hat{S}_F^{(l,new\_p^*(l))}$ and $new\_p^*(l)$ has higher preference than $p^*(l)$ ($\psi^{(l,new\_p^*(l))}>\psi^{(l,p^*(l))}$) (line 8). Finally, as reflected in the condition of line 9, an SpHO is also performed if $p^*(l)$ is no longer available to link l after being reassigned to another active link in the previous iterations of the loop of line 5. Once all active links are explored, the list of assigned pools is updated to consider all SpHOs that need to be performed as a result of the algorithm (line 16).

Algorithm 2 Fittingness Factor-based SS

1: **if** link l establishment request **then**
2: **if** $Av\_Pools=\emptyset$ **then**
3: Reject request;
4: **else**
5: Get $\{\hat{S}_F^{(l,p)}\}_{1\leq p\leq P}$ from the KM;
6: Compute $g\left(\hat{S}_F^{(l,p)}(t), T_{req,l}\right)$ for all pools;
7: $p^*(l) \leftarrow \arg\max_{p\in Av\_Pools}\left(g\left(\hat{S}_F^{(l,p)}(t), T_{req,l}\right)\right)$;
8: **end if**
9: **end if**

Algorithm 3 Fittingness Factor-based SM

1: **if** (link l^* release) OR (change in any active $\hat{S}_F^{(l^*,p^*)}$) **then**
2: Get $\{\hat{S}_F^{(l,p)}\}_{1\leq L\leq l, 1\leq p\leq P}$ from the KM;
3: $New\_Assigned \leftarrow \emptyset$;
4: Sort $A(t)$ in the decreasing order of $R_{req,l}/\overline{R_l}$;
5: **for** $l = 1 \rightarrow |A(t)|$ **do**
6: $new\_p^*(l) \leftarrow \arg\max_{p\in Av\_Pools}\left(g\left(\hat{S}_F^{(l,p)}(t), Rem\_T_l(t)\right)\right)$;
7: **if** $((\hat{S}_F^{(l,p^*(l))}=LOW)$ AND $(\hat{S}_F^{(l,new\_p^*(l))}=HIGH))$ OR
8: $((\hat{S}_F^{(l,p^*(l))}=\hat{S}_F^{(l,new\_p^*(l))})$ AND $(\psi^{(l,new\_p^*(l))}>\psi^{(l,p^*(l))}))$ OR
9: $(p^*(l)\in new\_Assigned)$ **then**
10: $p^*(l) \leftarrow new\_p^*(l)$;
11: $New\_Assigned \leftarrow New\_Assigned \bigcup \{new\_p^*(l)\}$;
12: **else**
13: $New\_Assigned \leftarrow new\_Assigned \bigcup \{p^*(l)\}$;
14: **end if**
15: **end for**
16: $Assigned \leftarrow New\_Assigned$;
17: **end if**

V. Applicability Example: The Future Digital Home

To evaluate the effectiveness of the proposed framework in assisting in the spectrum management decision-making process, a realistic DH environment similar to that of [27] is considered. The DH environment offers new opportunities to improve efficiency through provisioning new management services [27]. The future DH is expected to consist of not only computing devices with communication capabilities (e.g., desktop PCs, laptops and the like), but also of consumer electronics (e.g., TV sets with wireless interfaces, digital media servers, camcorders, game consoles, home security and automation systems), as well as more traditional appliances (e.g., washing machines and fridges) equipped with communication interfaces to enable, for example, remote control and monitoring. The provisioning of wireless management services in the DH requires an efficient exploitation of all possible sources of available spectrum resources, e.g., license-exempt access to ISM bands, opportunistic access to UHF bands (i.e., TV white spaces) through e.g., the ECMA-392 radio networking standard [28] and also the exploitation of licensed spectrum (e.g., spectrum licensed to a mobile network operator providing management services in the DH) as a mechanism for enhancing QoS provision of some DH connections.

A. Considered Environment

The considered indoor environment is a single floor of dimensions 16.8 *m*×30.4 *m* organized in six different rooms, where a set of L radio links need to be established from co-located transmitters to DH node receivers that may be located anywhere in the floor plan shown in Fig. 3(a). The following P=3 candidate spectrum pools are considered:

- Pool #1: BW_1=20 *MHz* bandwidth in the 2.4 *GHz* ISM license-exempt band;
- Pool #2: BW_2=16 *MHz* bandwidth in the 600 *MHz* TV White Space (TVWS) band that can be operated opportunistically;
- Pool #3: BW_3=20 *MHz* bandwidth in a 2.6 *GHz* licensed band of the Mobile Network Operator (MNO) serving as the DH management service provider.

The radio and interference conditions experienced in these pools are described as follows:

- Radio propagation losses experienced at DH receivers are modeled using the COST 231 model [29] that is given by:

$$L(dB) = L_0 + 20\log f(Mhz) + 10\alpha_P \log d(m) + N_w \times L_w \quad (24)$$

where L_o=−27.55 dB, α_P is the propagation coefficient at distance $d(m)$, N_w is the number of traversed walls between communicating parties and L_w is the attenuation of one wall that depends on its material and width. Based on the measurements performed in [27], the propagation model can be properly tuned to the considered indoor environment by setting σ_p=2.6 and L_w=5.1 *dB*.
- The transmitted power is assumed to be 20 *dBm* in all three pools.

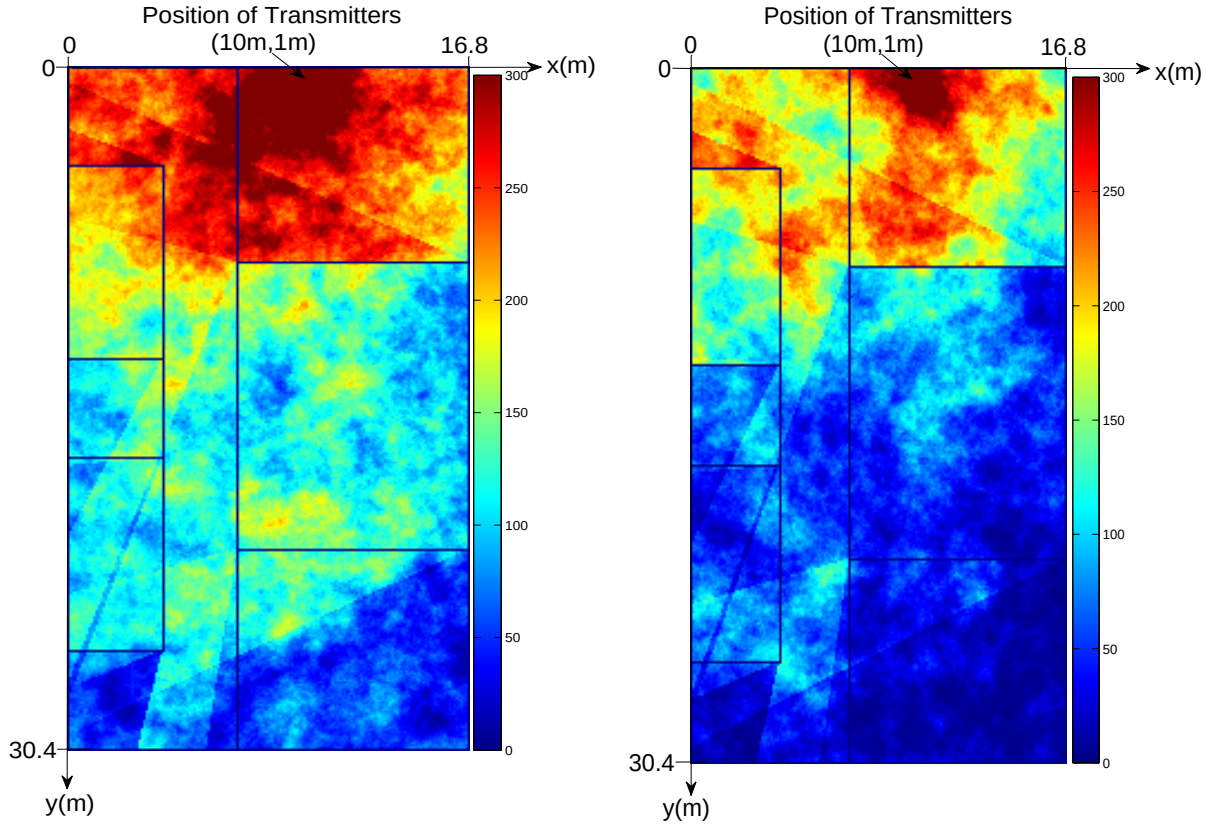

(a) in the low-interference state I_0

(b) in the high-interference state I_1

Fig. 3. Achievable bit-rates (Mbit/s) with pool #1

- To characterize the presence of external interferers, a simple interference model that captures the most relevant features affecting SS has been retained. In this respect, a heterogeneous interference situation is considered in which the sum of the noise and interference power spectral density $I(p)$ experienced in each pool $p\in\{1,..,P\}$ follows a two-state discrete time Markov chain jumping between a state of low interference $I_0(p)$ and a state of high interference $I_1(p)$ with transition probabilities $P_{01}(p)$ (i.e., probability of moving from state I_0 to I_1 in one simulation step) and $P_{10}(p)$ (i.e., probability of moving from state I_1 to I_0). It is assumed that the evolution of external interference is not affected by the activity of established links in the considered DH environment and the associated decisions of the spectrum selection framework.
- Based on these probabilities, the average durations of the $I_0(p)$ and $I_1(p)$ states are, respectively, given by:

$$\overline{I_0(p)}=\frac{1}{P_{01}(p)} \tag{25}$$

$$\overline{I_1(p)}=\frac{1}{P_{10}(p)} \tag{26}$$

- In our specific case, it is assumed that pools #1 and #2 alternate between $I_0(p)$ and $I_1(p)$ randomly with transition probabilities of $P_{10}(1)$=$55.5\cdot10^{-5}$ and $P_{01}(1)$=$3.7\cdot10^{-5}$ for pool #1 and $P_{10}(2)$=$833.33\cdot10^{-5}$ and $P_{01}(2)$=$55.5\cdot10^{-5}$ for pool #2. Based on these probabilities, the average durations of the low interference state for pools #1 and #2 are $\overline{I_0(1)}$=7.5 *h* and $\overline{I_0(2)}$=0.5 *h*, respectively, while the average durations of the high interference state for pools #1 and #2 are $\overline{I_1(1)}$=30 *min* and $\overline{I_1(2)}$=2 *min*, respectively. In turn, pool #3, relying on the licensed-band operator interference control mechanisms, is assumed to be always free of interference.
- External interferers of pools #1 and #2 are assumed to transmit with power P=10 *dBm* and P=20 *dBm* in the low and high interference states, respectively. They are located at coordinates (30 *m*, 15 *m*) and (−12.2 *m*, 15 *m*), respectively (see Fig. 4).

The proposed model properly captures the richness of the considered DH environment and the diverse radio and interference conditions that may be experienced within it. As illustrative example, Fig. 3(a) and Fig. 3(b) represent a spatial map of the Shannon-bound achievable bit rates (Mbit/s) using pool #1 in the low and high interference states, respectively. The map clearly illustrates the extent to which interference conditions affect the achievable bit rates in each position.

Performance is evaluated considering L=2 radio links placed in the positions shown in Fig. 4 under the following assumptions:

- The link #1 receiver is situated in a fixed position, while the link #2 receiver may jump between the positions #0 and #1 indicated in Fig. 4. Link #1 is associated with low-data-rate sessions ($R_{req,1}$=20 *Mbps* and $T_{req,1}$=2 *min*), while link #2 is associated with high-data-rate

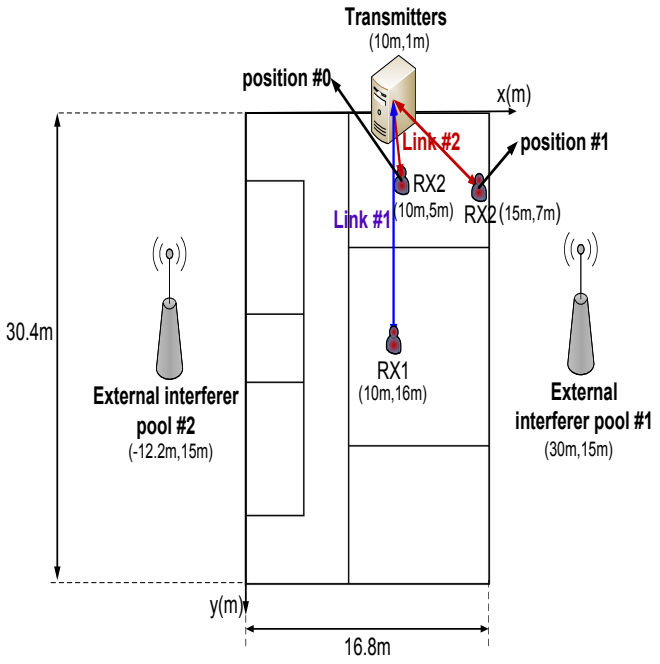

Fig. 4. Positions of the different links

sessions ($R_{req,1}$=200 *Mbps* and $T_{req,1}$=20 *min*).

- The l-th link generates sessions with constant duration $T_{req,l}$ and inactivity periods exponentially distributed with average $1/\lambda_l$ for each link $l\in\{1,2\}$.
- To smooth the short-term variability of interference conditions, $R(l,p)$ values experienced within each of the $I_0(p)$ and $I_1(p)$ states are averaged. The average bit rates achievable in the different pools are presented in Table I.
- The preference factors are $\psi^{(l,1)}$=$\psi^{(l,2)}$=0.9 and $\psi^{(l,3)}$=0.1, $l\in\{1,2\}$. This configuration reflects that the DH communication manager aims at limiting the use of the MNO band by exploiting as much as possible either the ISM or TVWS bands.

The system is observed in time steps of 1 s till establishing $65,000$ sessions for each link. The other simulation parameters are ξ=5, $\delta_{l,p}$=0.5, η_L=0, η_H=1, ρ=0.25, γ=0.95, α_{max}=0.05, M=6, T_Inact=10 h, and N=200.

B. Model of non-stationary conditions

To assess robustness to changes in the radio and interference conditions of the different spectrum pools, it is assumed that the position of the link #2 receiver may jump during system operation between the two positions indicated in Fig. 4 according to one of the following changes:

- $Change$ #1: the link #2 receiver is initially placed in position #0, and then moved to position #1.
- $Change$ #2: the link #2 receiver placed in position #1 is moved back to position #0.

Unlike position #0, where both LOW and HIGH fittingness factor states are observed by link #2 using pool #1 in the high and low interference states, respectively, position #1 is so close to the external interferer of pool #1 that only the LOW state is observed regardless of interference conditions.

C. Benchmarking

To assess the influence of the different components of the proposed framework, the following variants will be compared:

- *SS+SM*: This approach makes use of both the SS and SM algorithms, but does not include the RT to detect possible changes and regenerate KD statistics in case.
- *SS+SM+RT*: This is the complete approach that includes the SS, SM and RT functionalities.

Apart from the considered variants, the following reference schemes are introduced for benchmarking purposes:

- *Rand*: This implements only the spectrum selection module of Fig. 2 and performs a random selection among available pools. None of the KM, SM and RT modules is used.
- *Optim*: This scheme solves, in each simulation step, the optimization problem of (8) and performs the required reconfigurations to use the best combination of pools and active links. The computation of the optimum has been carried out based on an exhaustive search, which is computationally feasible in the considered scenario.

D. Performance Indicators

The reliability of the proposed strategy in solving the considered optimization problem is analysed using the following metric:

- $\overline{f(d_{l,p}(t))}$: Average utility perceived by active links. It is computed by averaging over time the values of the objective function $f(d_{l,p^*(l)}(t))$ defined in (9).

To analyze the different factors influencing $\overline{f(d_{l,p}(t))}$, the following KPIs are considered:

- $Dissf(l,p)$: Dissatisfaction probability of link l in using pool p, defined as

$$Dissf(l,p)=Prob\left[R(l,p)<R_{req,l}\right] \tag{27}$$

- $Usage(l,p)$: Fraction of time for which pool p is used by link l sessions.
- $Regret(l,p)$: Regret of link l in using pool p to capture the fulfillment of pool preference constraints. It is defined as the probability that there exists another available pool p' able to equally fulfill the bit rate requirements of link l with higher preference than pool p, weighted by $Usage(l,p)$, that is:

$$\begin{aligned} Regret(l,p)=&Usage(l,p)\cdot Prob[\exists p'\in Av\_Pools,\\ &(R(l,p')>R_{req,l})AND(R(l,p)>R_{req,l})\\ &AND(\psi^{(l,p')}>\psi^{(l,p)})] \end{aligned} \tag{28}$$

- $Fairness(t)$: The Jains fairness index based on utilities defined at a given time t as follows [30]:

$$Fairness(t)=\frac{\sum_{l\in A(t)}\left(u^{(l,p)}(t)\right)^2}{|A(t)|\cdot\left(\sum_{l\in A(t)}u^{(l,p)}(t)\right)^2} \tag{29}$$

Note that $Fairness(t)$ assesses whether active links are receiving a fair share of utilities with values ranging from 0 (unfair) to 1 (fair).

TABLE I
AVERAGE ACHIEVABLE BIT RATES (MBPS)

	pool #1		pool #2		pool #3
	State I_0	State I_1	State I_0	State I_1	State I_0
Link #1	88.8	32.5	106.6	55.45	229.3
Link #2 (position #0)	228	161.9	244.2	191.2	361.7
Link #2 (position #1)	157.7	92.4	239.8	187.2	285.6

Furthermore, practicality of the proposed solution is assessed based on the following KPIs:

- *Nb. SpHOs/session*: The average number of SpHOs performed per link session.
- *Nb. Reports/s*: The average number of measurement reports sent per second.

Finally, the procedure of detecting changes described in Section IV.A-3 is performed by the RT based on monitoring the following 3 KPIs for each link l (which yields a total of $M{=}3L{=}6$ KPIs):

- The average dissatisfaction probability, $Dissf(l)$.
- The average number of SpHOs performed per session, $SpHO(l)$.
- The average fraction of using pool #3, $Usage(l,3)$.

VI. RESULTS

A. Performance evaluation

This section presents the performance evaluation of the different schemes introduced in Section V-C. For the sake of simplicity, the model of non-stationary conditions described in Section V-B is initially not considered. In this respect, it is assumed that DH receivers are kept in the fixed positions shown in Fig. 4 with the link #2 received placed in position #0, and that interference conditions remain stationary, which means that *SS+SM+RT* is equivalent to *SS+SM*.

Fig. 5(a) plots the average utility $\overline{f(d_{l,p}(t))}$ achieved by all considered schemes as a function of the total offered traffic load in bits per second (bps) defined as

$$\textit{Offered Traffic (bps)} = \sum_{l} \theta_l \cdot R_{req,l} \qquad (30)$$

where $\theta_l{=}\lambda_l{\cdot}T_{req,l}$ denotes the offered traffic load to link l in Erlang.

For a better analysis of the impact of the different factors influencing $\overline{f(d_{l,p}(t))}$, Fig. 5(b) and Fig. 5(c) plot the dissatisfaction probability of link #2 ($Dissf(2)$) and the regret of link #2 in using the least preferred pool #3 ($Regret(2,3)$), respectively. Results for link #1 are not presented because it is always satisfied (i.e., the bit rate is always above the requirement of 20 *Mbps*) and it never uses pool #3. Finally, to analyze the share of the total utility among active links, Fig. 5(d) plots the average fairness index ($\overline{Fairness(t)}$) achieved by the proposed strategy (*SS+SM+RT*) with respect to the *Optim* and *Rand* schemes.

The results in Fig. 5(a) indicate that the proposed strategy (*SS+SM+RT*) strongly outperforms *Rand* in terms of $\overline{f(d_{l,p}(t))}$ (gains up to 45%) and approximates very well the optimal solution (*Optim*) for most traffic loads. This is because, on the one hand, the estimated states $\hat{S}_F^{(l,p)}$ provided by the KM together with the use of SM contribute to assigning the most suitable pools to link #2 sessions, which reduces the risk of being dissatisfied as reflected in Fig. 5(b). On the other hand, the prioritization of pools #1 and #2 tends to avoid using pool #3 as much as possible, which significantly improves the regret of using it (see Fig. 5(c)). Note that the small deviation observed in $\overline{f(d_{l,p}(t))}$ for low traffic load is mainly due to the slight loss in the regret of using pool #3 observed in Fig. 5(c). The analysis of the fairness behavior in Fig. 5(d) indicates that $\overline{Fairness(t)}$ is close to 1 for both *SS+SM+RT* and *Optim*, while it significantly decreases for *Rand* as traffic load increases.

Therefore, the proposed *SS+SM+RT* strategy provides a good approximation of the optimal solution of (8) for most traffic loads, mainly thanks to the support of the KM and SM components.

B. Practicality of the proposed solution

This section assesses the practicality of the proposed strategy (*SS+SM+RT*) with respect to the optimal scheme (*Optim*) in terms of signaling requirements at the air interface.

Fig. 6(a) plots the number of measurement reports sent per second (*Nb. Reports/s*) by *SS+SM+RT* and *Optim* with a vertical axis in logarithmic scale for improved visualization. Fig. 6(b) plots the corresponding average number of SpHOs per session (*Nb. SpHOs/session*).

The results indicate that *SS+SM+RT* significantly outperforms *Optim* in terms of both *Nb. Reports/s* (Fig. 6(a)) and *Nb. SpHOs/session* (Fig. 6(b)).

On the one hand, the gain in terms of *Nb. Reports/s* is justified by the capability of *SS+SM+RT* to exploit the previous experience of using inactive link/pool pairs. As a matter of fact, spectrum decisions depend only on the $\hat{S}_F^{(l,p)}$ estimates determined by the KM based on previous measurements of $R(l,p)$. Therefore, only measurements on active link/pools are generated by *SS+SM+RT*. On the contrary, *Optim* requires to know the exact $S_F^{(l,p)}$ states of all pools to continuously solve (8). Therefore, $R(l,p)$ values of the different pools should be measured and reported even when pools are not used, which results in the significant increase in *Nb. Reports/s* observed in Fig. 6(a) with respect to *SS+SM+RT*.

On the other hand, the better SpHO performance is because the proposed strategy performs pool reconfigurations only when a significant gain in the utility $u^{(l,p)}$ can be obtained. Specifically, SpHOs are executed only when the state $\hat{S}_F^{(l,p)}$ of the pool in use goes from LOW to HIGH or when a pool that provides a higher preference factor $\psi^{(l,p)}$ can be used

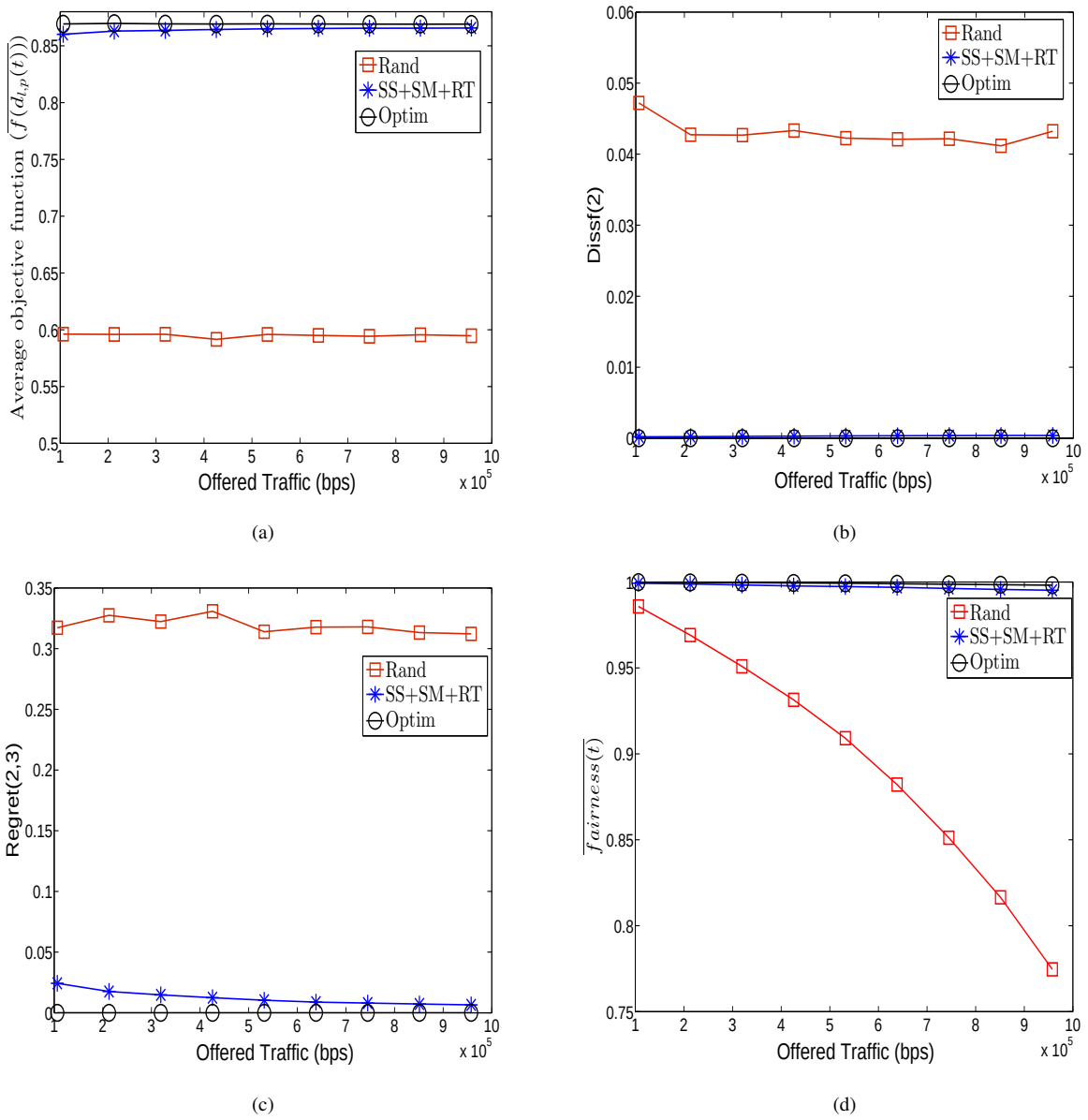

Fig. 5. Analysis of SS performance in terms of (a) $\overline{f(d_{l,p}(t))}$, (b) $Dissf(2)$, (c) $Regret(2,3)$ and (d) Average Fairness index.

as specified in lines 7-8 of Algorithm 3, respectively. When one of these conditions holds, a significant gain in the utility $u^{(l,p)}$ can be achieved by performing an SpHO. On the contrary, *Optim* reassigns pools whenever the objective function $f(d_{l,p}(t))$ given by (9) can be increased. Nevertheless, the gain in $f(d_{l,p}(t))$ may be very small particularly when switching between pools #1 and #2 associated with equal preference factor ($\psi^{(l,1)}$=$\psi^{(l,2)}$=0.9) and similar average fittingness factor values. Therefore, *Optim* performs many additional pool reconfigurations compared to *SS+SM+RT* with a minor gain in $f(d_{l,p}(t))$ as previously observed in Fig. 5(a).

In summary. the proposed strategy approximates very well the optimal solution of the considered problem in (8) with less reconfiguration and reporting events, which strongly supports its practicality.

C. RT capability to detect changes

This section evaluates the capability of the RT to detect relevant changes in the radio and interference conditions of the different spectrum pools. The first position change described in Section V-B ($Change\ \#1$) is considered for illustrative purposes. It occurs after establishing $9,750$ sessions for each link.

Fig. 7(a) plots the temporal evolution of the initial RT estimate of the number of SpHOs/session for link #2 ($\overline{SpHO(2)}$) with the corresponding confidence interval shown in dashed lines. Only link #2 sessions are considered with θ_2=0.9 Er for better analysis of system reactivity because link #1 is always satisfied. The time evolution on the x-axis is shown in terms of the number of established link #2 sessions according to the generation process described in Section V-A. Note that only $SpHO(2)$ is considered because this is the KPI for which

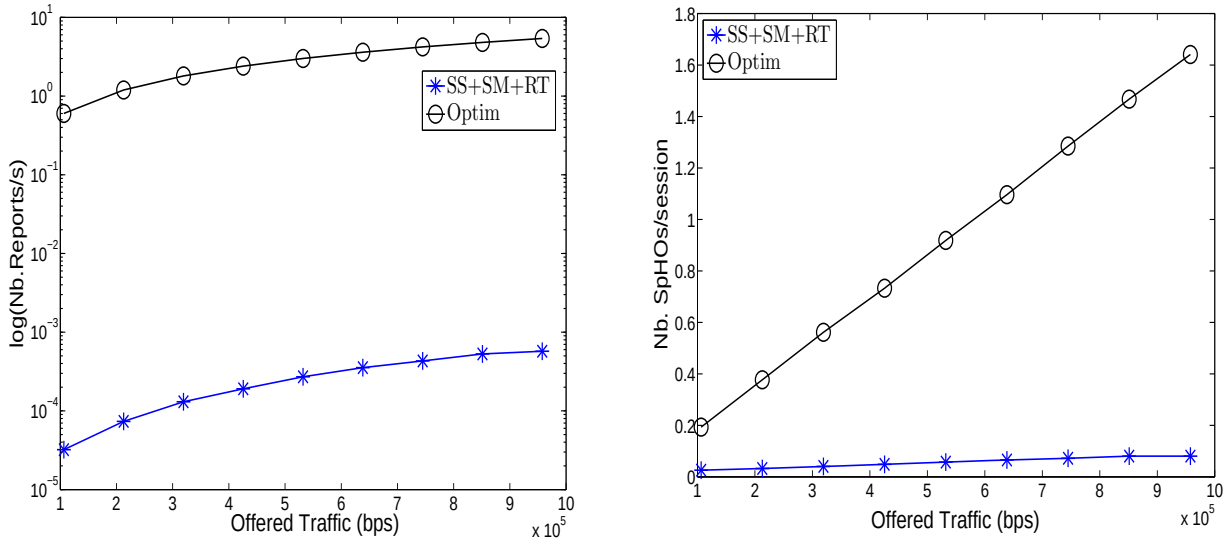

(a) (b)

Fig. 6. Practicality of $SS{+}SM{+}RT$ in terms of (a) $Nb.Reports/s$ and (b) *Nb. SpHOs/session*.

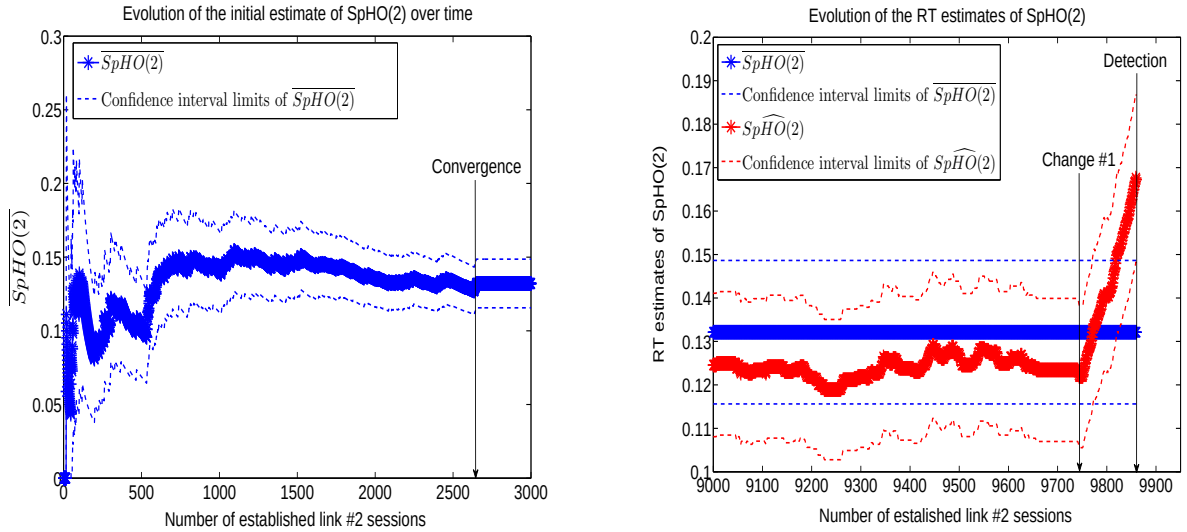

(a) (b)

Fig. 7. Evolution of the RT estimates of $SpHO(2)$ (a) initially and (b) around the considered change.

H_1 is selected by the RT after the change occurs.

The results show that $\overline{SpHO(2)}$ tends to converge as more link #2 sessions are established. Specifically, the stopping rule of (17) is met after establishing around $2,650$ sessions. At this point of time, the initial $\overline{SpHO(2)}$ estimate and its confidence interval are frozen, and the RT starts to monitor the second moving-average estimate ($\widehat{SpHO(2)}$).

Fig. 7(b) plots the temporal evolution of $\widehat{SpHO(2)}$ and its corresponding confidence interval around the considered change. The initial estimate $\overline{SpHO(2)}$ is also shown for comparison purposes. The results show that, before the change occurs, the moving average estimate $\widehat{SpHO(2)}$ oscillates close to $\overline{SpHO(2)}$ due to the intrinsic randomness of radio conditions. Nevertheless, the RT disregards these oscillations and selects H_0 because confidence intervals of the two estimates are still overlapping. After $Change\,\#1$ occurs, $\widehat{SpHO(2)}$ starts to deviate much from $\overline{SpHO(2)}$ till their confidence intervals no longer overlap. At this moment, H_1 is selected for $SpHO(2)$ and the considered change is detected by the RT. It is worth mentioning that only two wrong changes (Type I errors) are detected during the whole simulation, which corresponds to $Type\,I\,error{=}3.2{\cdot}10^{-5}$. This much smaller value compared to α_{max} is because, on the one hand, only $M{=}6{<}M_{max}{=}8$ KPIs have been used. On the other hand, the individual tests associated with the considered KPIs are dependent since a change in interference conditions has a joint impact on all KPIs. Therefore, a much better performance can be achieved with respect to the conservative Bonferroni correction as previously explained Section IV-A3.

In summary, the RT probabilistic detector, based on hypothesis testing, enables to filter those changes related to the

intrinsic randomness of the radio environment and efficiently detect relevant changes in the scenario.

D. Robustness analysis

This section evaluates robustness of the proposed strategy when the initial radio and interference conditions, under which the KD statistics were generated, no longer hold. For that purpose, the two possible changes in the position of link $\#2$ receiver, described in Section V-B, are introduced in two different simulations.

Let us consider first $Change\ \#1$ in which the receiver is moved to a position with worse interference conditions for pool $\#1$. Fig. 8(a) shows the online evolution of the dissatisfaction level of link $\#2$ ($Dissf(2)$). The time evolution on the x-axis is shown in terms of the number of established link $\#2$ sessions according to the generation process described in Section V-A with the position change occurring after $9,750$ sessions. To analyze the impact of RT, both *SS+SM* and *SS+SM+RT* variants are considered. Once again, only link $\#2$ sessions are considered with θ_2=$0.9\ Er$ for better analysis of system reactivity. Fig. 8(b) and Fig. 8(c) plot the corresponding number of SpHOs per session and regret in using pool $\#3$, respectively.

The results show that, after $Change\ \#1$, both *SS+SM* and *SS+SM+RT* result in worse performance in terms of $Dissf(2)$ and *Nb. SpHOs/session*. As the number of established sessions increases, both statistics tend to converge to larger values than those obtained prior to the change. The observed degradation is because after the change, the new position $\#1$ is too close to the external interferer of pool $\#1$, thus making it useless regardless of interference conditions (i.e., providing always a LOW $S_F^{(l,p)}$). Nevertheless, the use of the RT functionality (*SS+SM+RT*) results in much smaller degradation. The reason for this better performance is that, after the position change, the strategy *SS+SM* without any support from the RT still relies on the out-of-date KD statistics previously generated in position $\#0$, so it may decide in some cases to assign pool $\#1$ to link $\#2$ sessions. However, this turns out to be a wrong allocation because, in the new position $\#1$, pool $\#1$ has always a LOW $S_F^{(l,p)}$ regardless of its interference conditions. Correspondingly, this degrades the dissatisfaction probability (see Fig. 8(a)). In addition, much more frequent SpHOs are required to change pool $\#1$ whenever it is assigned (Fig. 8(b)). On the contrary, when RT is used (*SS+SM+RT*), new KD statistics are generated in position $\#1$ after detecting $Change\ \#1$. As a consequence, the estimate $\hat{S}_F^{(l,p)}$ of pool $\#1$ is always set to LOW, and pool $\#1$ is never assigned in the future to link $\#2$. This results in the significant gain observed in both the dissatisfaction level (Fig. 8(a)) and number of performed SpHOs (Fig. 8(b)).

In Fig. 8(c), it can be observed that the regret of using pool $\#3$ performs similarly for both strategies before and after the change. Before the change, either pool $\#1$ or $\#2$ can be allocated because their $\hat{S}_F^{(l,p)}$ states alternate between LOW and HIGH. This marginalizes the risk of unnecessarily using the least preferred pool $\#3$ because it is not likely to wrongly set the $\hat{S}_F^{(l,p)}$ estimate of both pools to LOW, which would lead to an unnecessary assignment of pool $\#3$. Then, after the change, the use of pool $\#1$ is excluded by both strategies (at first assignment for *SS+SM+RT* or after initially assigning it, and then executing an SpHO for *SS+SM*). As a consequence, whenever the $\hat{S}_F^{(l,p)}$ estimate of pool $\#2$ is wrongly set to LOW, pool $\#3$ will be unnecessarily assigned with the corresponding increase in the regret that can be observed in Fig. 8(c) after the change.

Focusing now on $Change\ \#2$, Fig. 9(a) shows the online evolution of the dissatisfaction level of link $\#2$ with the position change occurring after $9,750$ sessions. The number of SpHOs per session and regret in using pool $\#3$ are plot in Fig. 9(b) and Fig. 9(c), respectively.

The results show that after $Change\ \#2$, the use of RT functionality results in a significant reduction of both the dissatisfaction level (Fig. 9(a)) and the number of performed SpHOs (Fig. 9(b)). This is because pool $\#1$, which is initially not used in position $\#1$, becomes often the most suitable pool for link $\#2$ after the RT detects the position change and the new KD statistics are regenerated in the new position. On the contrary, when the RT is not supported (*SS+SM*), $Change\ \#2$ has no impact on the observed dissatisfaction level (Fig. 9(a)) and number of SpHOs (Fig. 9(b)) because link $\#2$ continues to exclude pool $\#1$ based on the old KD statistics. In contrast to *SS+SM+RT*, this results in penalizing the regret of using pool $\#3$ whenever this pool is assigned instead of pool $\#1$ (see Fig. 9(c)).

VII. Conclusions

This paper has proposed a new knowledge management framework for SS under non-stationary conditions supporting a set of applications with heterogeneous requirements. In this respect, an optimization problem has been formulated to maximize an aggregate utility function that jointly captures the suitability of spectrum portions in terms of fittingness factors that measure the capacity of each spectrum pool in relation to the bit rate requirements of the applications, and a set of preference factors for utilizing the different spectrum bands. To tackle the considered problem in a practical way, the proposed framework relies on a KM that exploits a statistical characterization of the environment stored in a KD to monitor the time-varying suitability of spectrum resources and drive the spectrum management decision-making process accordingly. To support non-stationary environments, a RT has been developed to detect, based on hypothesis testing, relevant changes in the scenario subject to the intrinsic randomness of radio conditions and perform, when needed, the required updates. Then, a novel strategy combining SS and SM functionalities has been proposed to efficiently solve the considered problem. Analysis in a realistic DH environment has revealed that the proposed strategy approximates very well the optimal solution in terms of achieved utility values, by assigning the most suitable pools to the different link sessions while minimizing usage of the least preferred pools. An analysis of the practicality in terms of signaling requirements has revealed that the proposed strategy exploits the estimated suitability levels provided by the KM and the event-based triggering

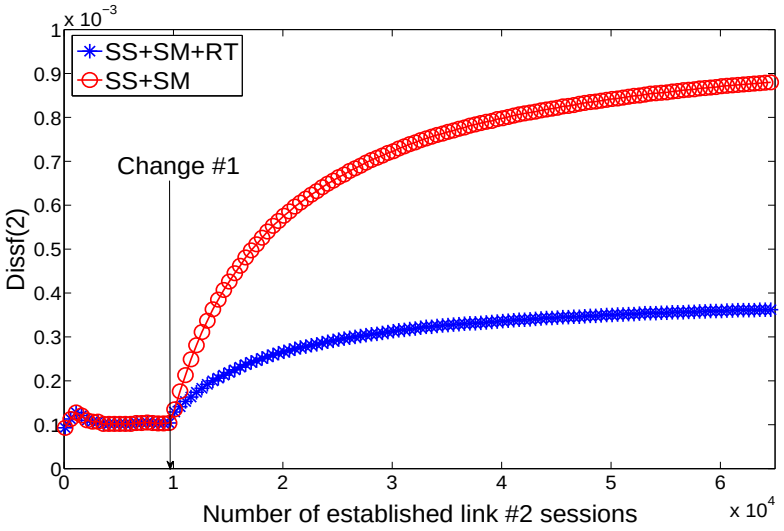

(a)

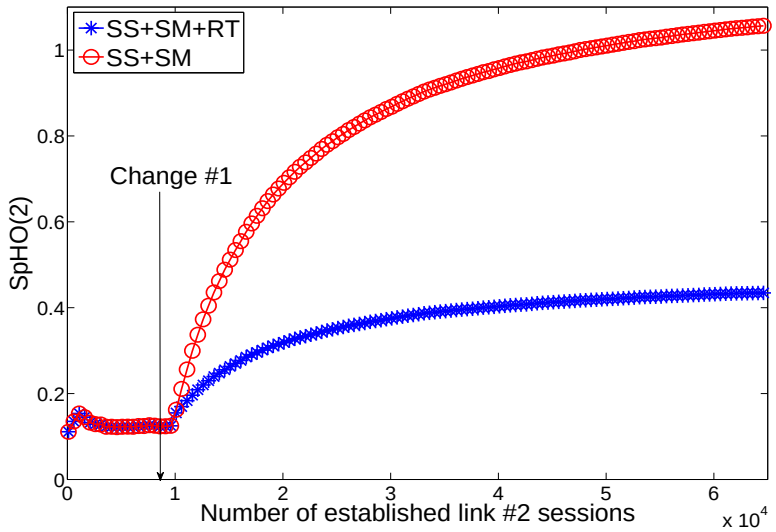

(b)

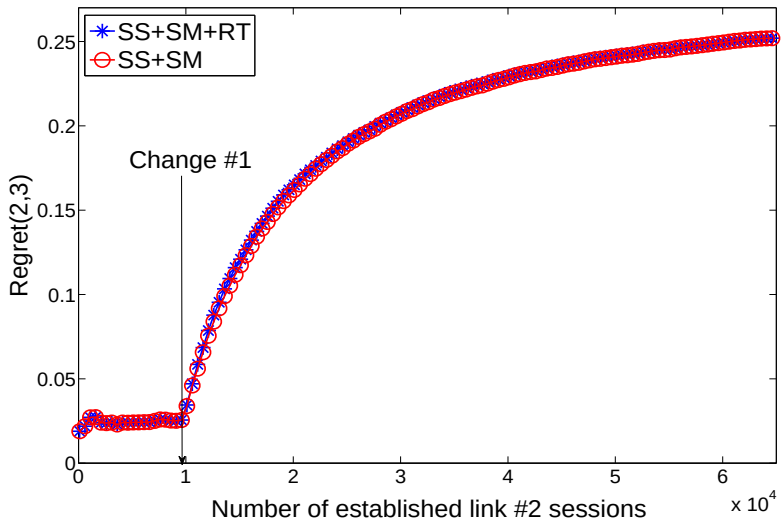

(c)

Fig. 8. Online evolution of (a) $Dissf(2)$, (b) *Nb. SpHOs/session* and (c) $Regret(2,3)$ with $Change\ \#1$ occurring after $9,750$ sessions.

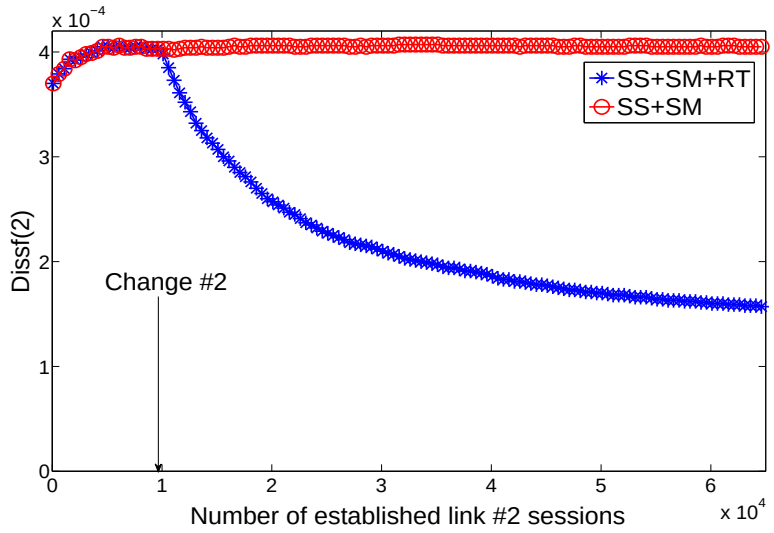

(a)

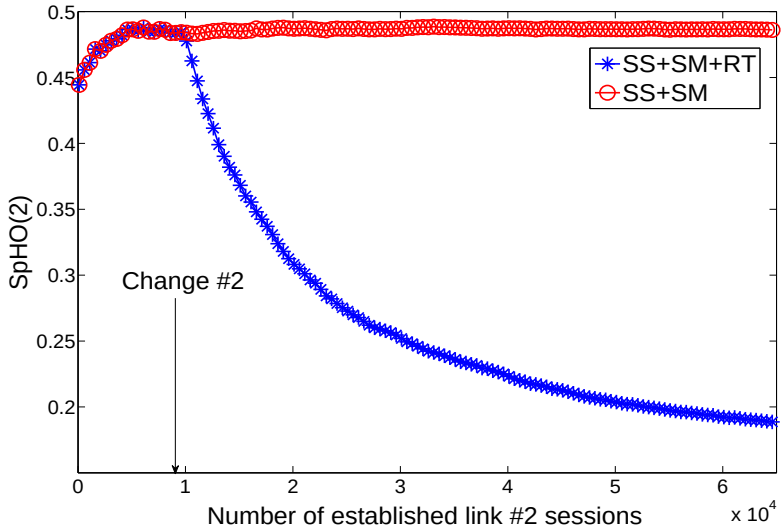

(b)

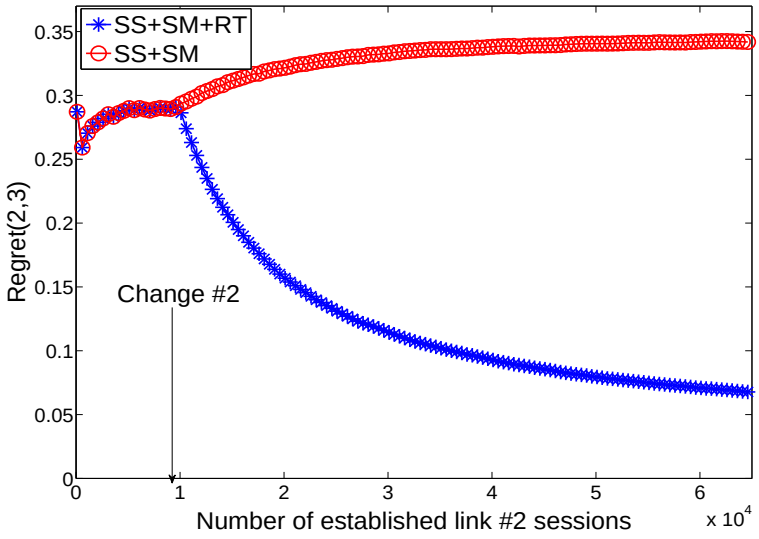

(c)

Fig. 9. Online evolution of (a) $Dissf(2)$, (b) *Nb. SpHOs/session* and (c) $Regret(2,3)$ with $Change\ \#2$ occurring after $9,750$ sessions.

of SM to significantly reduce the amount of measurement reporting and pool reconfigurations, respectively, with respect to the optimal solution. An analysis of robustness under non-stationary conditions has revealed that the proposed RT is able to exploit the probabilistic detection rule of hypothesis testing to filter most of changes due the intrinsic radio randomness and detect actual changes in the scenario. Thanks to the RT support, the proposed spectrum management strategy exhibits substantial robustness in front of unexpected changes, thus showing the practicality of the proposed strategy in such realistic environments.

APPENDIX A
ESTIMATION OF CONDITIONAL PROBABILITIES OF FITTINGNESS FACTOR STATES

Assuming that we know the fittingness factor state at time $t-\Delta t^{(l,p)}$ ($S_F^{(l,p)}(t-\Delta t^{(l,p)})$) and considering the definition of the $\boldsymbol{x_F^{(l,p)}(t-\Delta t^{(l,p)})}$ vector in (7), the vector of conditional probabilities of fittingness factor states at the next time unit $t-\Delta t^{(l,p)}+1$ is given by:

$$\boldsymbol{\Pi_{F|F}^{(l,p)}(t-\Delta t^{(l,p)}+1,1)=T_F^{(l,p)^T}\cdot x_F^{(l,p)}(t-\Delta t^{(l,p)})} \tag{31}$$

Iterating the above expression k times, it is easy to obtain that, for a given instant $t-\Delta t^{(l,p)}+k$, it yields

$$\boldsymbol{\Pi_{F|F}^{(l,p)}(t-\Delta t^{(l,p)}+k,k)=\left[T_F^{(l,p)^T}\right]^k\cdot x_F^{(l,p)}(t-\Delta t^{(l,p)})} \tag{32}$$

Then, by considering $k=\Delta t^{(l,p)}$, the expression (12) is obtained.

APPENDIX B
ANALYSIS OF THE TYPE I AND II ERRORS OF THE OVERLAP DETECTION METHOD

The asymptotic Type I and II errors of the overlap detection method are given by [25]:

$$Type\ I\ error=2\phi\left(\frac{z_{(1-\gamma)/2}(1+k_m)}{\sqrt{1+k_m^2}}\right) \tag{33}$$

$$\begin{aligned} Type\ II\ error=&1-\phi\left(\frac{z_{(1-\gamma)/2}(1+k_m)}{\sqrt{1+k_m^2}}+D_m\right)\\ &-\phi\left(\frac{z_{(1-\gamma)/2}(1+k_m)}{\sqrt{1+k_m^2}}-D_m\right)\end{aligned} \tag{34}$$

Fig. 10 plots Type I and II errors as a function of the ratio of sample variances k_m. Different values of D_m are considered for the Type II error. It can be seen that for high D_m and low k_m values, the overlap detection method provides a very low Type I error (e.g, 0.0056 for k_m=1) and an acceptable Type II error (e.g, 0.013 for k_m=1 and D_m=5). Therefore, it provides a good option to detect relevant changes in the environment while minimizing the risk of useless generation of KD data.

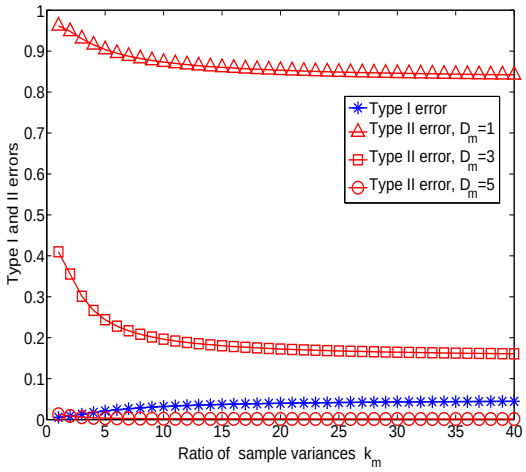

Fig. 10. The overlap detection Type I and II errors

APPENDIX C
ESTIMATION OF THE AVERAGE UTILITY ALONG SESSION DURATION

Given the estimated fittingness factor state at time t ($\hat{S}_F^{(l,p)}(t)$), the vector with the probabilities $\hat{\Pi}_{F|F,k}^{(l,p)}(t+1)=Prob\left[\hat{S}_F^{(l,p)}(t+1)=k|\hat{S}_F^{(l,p)}(t)\right]$ of being in each of the states k at time $t+1$ is given by:

$$\boldsymbol{\hat{\Pi}_{F|F}^{(l,p)}(t+1)=T_F^{(l,p)^T}\cdot\hat{x}_F^{(l,p)}(t)} \tag{35}$$

where $\hat{x}_F^{(l,p)}(t)$ is defined in (23).

Iterating the above expression k times, it yields

$$\boldsymbol{\hat{\Pi}_{F|F}^{(l,p)}(t+k)=\left[T_F^{(l,p)^T}\right]^k\cdot\hat{x}_F^{(l,p)}(t)} \tag{36}$$

Consequently, the expected utility at time $t+k$ is given by:

$$\begin{aligned} &E\left[u^{(l,p)}(t+k)|\hat{S}_F^{(l,p)}(t)\right]\\ &=\psi^{(l,p)}\cdot\overline{\boldsymbol{F^{(l,p)}}}^{\boldsymbol{T}}\cdot\boldsymbol{diag}[\eta_L,\eta_H]\cdot\boldsymbol{\hat{\Pi}_{F|F}^{(l,p)}(t+k)}\\ &=\psi^{(l,p)}\cdot\overline{\boldsymbol{F^{(l,p)}}}^{\boldsymbol{T}}\cdot\boldsymbol{diag}[\eta_L,\eta_H]\cdot\left[\boldsymbol{T_F^{(l,p)^T}}\right]^k\cdot\boldsymbol{\hat{x}_F^{(l,p)}(t)}\end{aligned} \tag{37}$$

By averaging (37) from k=1 up to the session duration $T_{req,l}$, the expression in (22) is obtained.

ACKNOWLEDGEMENTS

This work is supported by the Spanish Research Council and FEDER funds under ARCO grant (ref. TEC2010-15198) and by the Spanish Ministry of Science and Innovation (MICINN) under FPI grant BES-2009-017934.

REFERENCES

[1] J. Mitola III and G. Q. Maguire, Jr., "Cognitive radio: making software radios more personal," *Personal Communications, IEEE*, vol. 6, no. 4, pp. 13–18, Aug. 1999.

[2] S. Haykin, "Cognitive radio: brain-empowered wireless communications," *Selected Areas in Communications, IEEE Journal on*, vol. 23, no. 2, pp. 201–220, Feb. 2005.

[3] R. W. Thomas, D. H. Friend, L. A. Dasilva, and A. B. Mackenzie, "Cognitive networks: adaptation and learning to achieve end-to-end performance objectives," *Communications Magazine, IEEE*, vol. 44, no. 12, pp. 51 –57, Dec. 2006.
[4] J. Kephart and D. Chess, "The vision of autonomic computing," *Computer*, vol. 36, no. 1, pp. 41–50, Jan 2003.
[5] P. Demestichas, G. Dimitrakopoulos, J. Strassner, and D. Bourse, "Introducing reconfigurability and cognitive networks concepts in the wireless world," *Vehicular Technology Magazine, IEEE*, vol. 1, no. 2, pp. 32 –39, 2006.
[6] P. Demestichas, K. Tsagkaris, and V. Stavroulaki, "Cognitive management systems for supporting operators in the emerging Future Internet era," in *Personal, Indoor and Mobile Radio Communications Workshops (PIMRC Workshops), 2010 IEEE 21st International Symposium on*, sept. 2010, pp. 21 –25.
[7] E. Meshkova, Z. Wang, J. Nasreddine, D. Denkovski, C. Zhao, K. Rerkrai, T. Farnham, A. Ahmad, A. Gefflaut, L. Gavrilovska, and P. Mahonen, "Using cognitive radio principles for wireless resource management in home networking," in *Consumer Communications and Networking Conference (CCNC), 2011 IEEE*, jan. 2011, pp. 669 –673.
[8] The End-to-End-Efficiency (E3) project. [Online]. Available: https://www.ict-e3.eu/
[9] The ICT EU (Opportunistic Networks and Cognitive Management Systems for Efficient Application Provision in the Future InterneT) OneFIT Project. [Online]. Available: http://www.ict-onefit.eu/
[10] IEEE Standard Coordinating Committee 41 (SCC41). [Online]. Available: http://grouper.ieee.org/groups/scc41/index.html/
[11] ETSI Technical Committee (TC) on Reconfigurable Radio Systems (RRS). [Online]. Available: http://www.etsi.org/WebSite/technologies/RRS.aspx
[12] J. Vartiainen, M. Höyhtyä, J. Lehtomäki, and T. Bräysy, "Priority channel selection based on detection history database," in *crowncom, 2010*, June 2010, pp. 1–5.
[13] Y. Li, Y. Dong, H. Zhang, H. Zhao, H. Shi, and X. Zhao, "Qos provisioning spectrum decision algorithm based on predictions in cognitive radio networks," in *WiCOM 2010*, Sept. 2010, pp. 1–4.
[14] W.-Y. Lee and I. Akyldiz, "A spectrum decision framework for cognitive radio networks," *Mobile Computing, IEEE Transactions on*, vol. 10, no. 2, pp. 161–174, Feb. 2011.
[15] F. Bouali, O. Sallent, J. Pérez-Romero, and R. Agustí, "A framework based on a fittingness factor to enable efficient exploitation of spectrum opportunities in cognitive radio networks," in *Wireless Personal Multimedia Communications (WPMC), 2011 14th International Symposium on*, Oct. 2011, pp. 1–5.
[16] ——, "A fittingness factor-based spectrum management framework for cognitive radio networks," *Wireless Personal Communications*, pp. 1–15, 2013.
[17] The Faramir Project, "Flexible and spectrum aware radio access through measurements and modelling in cognitive radio systems, scenario definitions," Tech. Rep. D2.2, August 2010.
[18] ETSI, "Reconfigurable radio systems (RRS); use cases and scenarios for software defined radio (SDR) reference architecture for mobile device," Tech. Rep. TR 103 062, April 2011.
[19] ——, "Reconfigurable radio systems (RRS); use cases for operation in white space frequency bands," Tech. Rep. TR 102 907, November 2012.
[20] L. Badia, M. Lindström, J. Zander, and M. Zorzi, "Demand and pricing effects on the radio resource allocation of multimedia communication systems," in *GLOBECOM '03. IEEE*, vol. 7, Dec. 2003, pp. 4116–4121.
[21] J. E. Mitchell, "Branch-and-cut algorithms for combinatorial optimization problems," in *Handbook of Applied Optimization*. Oxford University Press, January 2002, pp. 65–77.
[22] "Reconfigurable Radio Systems, functional architecture for the management and control of reconfigurable radio systems," ETSI TR 102 682, Tech. Rep.
[23] One FIT Deliverable D2.2. (2011, February) Onefit functional and system architecture. [Online]. Available: http://www.ict-onefit.eu/
[24] E. L. Lehmann and J. P. Romano, *Testing statistical hypotheses*, 3rd ed., ser. Springer Texts in Statistics. New York: Springer, 2005.
[25] N. Schenker and J. F. Gentleman, "On judging the significance of differences by examining the overlap between confidence intervals," *The American Statistician*, vol. 55, no. 3, pp. pp. 182–186, 2001.
[26] R. J. Simes, "An improved Bonferroni procedure for multiple tests of significance," *Biometrika*, vol. 1, 1986.
[27] R. Ferrus, O. Sallent, J. Pérez-Romero, and R. Agustí, "A solution framework to provide management services for wireless communications in the digital home," *Communications Magazine, IEEE*, vol. 50, no. 11, pp. 132 –141, november 2012.
[28] ECMA, "MAC and PHY for operation in TV white space," Tech. Rep. ECMA-392, December 2009.
[29] COST, "Chapter 4, propagation prediction models," COST 231 Book, Tech. Rep. Final Report.
[30] R. K. Jain, D.-M. W. Chiu, and W. R. Hawe, "A quantitative measure of fairness and discrimination for resource allocation in shared computer systems," Digital Equipment Corporation, Tech. Rep., Sep 1984.

Faouzi Bouali received his telecommunication engineering degree (2004) and his masters degree in networks (2006) all with distinction from the Higher Communication School of Tunis (SUPCOM), Tunisia. From 2005 to 2009, he worked as radio optimization engineer within the Tunisian National Phone company where he was involved in many optimization projects of GSM/GPRS/EDGE/WCDMA networks. Since October 2009, has been pursuing his PhD degree within the Mobile Communication Research Group (GRCM) of the Dept. of Signal Theory and Communications (TSC) at the Universitat Politècnica de Catalunya (UPC) in Barcelona. His current research interests span the field of mobile radio-communication systems with a specific focus on efficient RRM algorithms, quality of service provisioning, and networking solutions for DSA (Dynamic Spectrum Access) networks.

Oriol Sallent is Full Professor at the Universitat Politècnica de Catalunya. His research interests are in the field of mobile communication systems, especially radio resource and spectrum management for cognitive heterogeneous wireless networks. He has published more than 150 papers in international journals and conferences. He has participated in several research projects of the 5th 6th and 7th Framework Programme of the European Commission and served as a consultant for a number of private companies.

Jordi Pérez-Romero is currently associate professor at the Dept. of Signal Theory and Communications of the Universitat Politècnica de Catalunya (UPC) in Barcelona, Spain. He received the Telecommunications Engineering degree and the PhD from the same university in 1997 and 2001. His research interests are in the field of mobile communication systems, especially packet radio techniques, radio resource and QoS management, heterogeneous wireless networks and cognitive networks. He has been involved in different European Projects as well as in projects for private companies. He has published papers in international journals and conferences and has co-authored one book on mobile communications. He is associate editor of IEEE Vehicular Technology Magazine and Eurasip Journal on Wireless Communications Networks.

Ramon Agustí received the Engineer of Telecommunications degree from the Universidad Politècnica de Madrid, Spain, in 1973, and the Ph.D. degree from the Universitat Politècnica de Catalunya (UPC), Spain, 1978. He became Full Professor of the Department of Signal Theory and Communications (UPC) in 1987. After graduation he was working in the field of digital communications with particular emphasis on transmission and development aspects in fixed digital radio, both radio relay and mobile communications. For the last fifteen years he has been mainly concerned with aspects related to radio resource management in mobile communications. He has published about two hundred papers in these areas and co-authored three books. He participated in the European program COST 231 and in the COST 259 as Spanish representative delegate. He has also participated in the RACE, ACTS and IST European research programs as well as in many private and public funded projects. He received the Catalonia Engineer of the year prize in 1998 and the Narcis Monturiol Medal issued by the Government of Catalonia in 2002 for his research contributions to the mobile communications field. He is a Member of the Spanish Engineering Academy.